

Tone Excitation of a Supersonic Bounded Shear Layer

Mahadevan Ramaswamy* and Eric Loth†

University of Illinois at Urbana-Champaign, Urbana, Illinois 61801-2935

Passive acoustic excitation was employed to augment mixing in a bounded planar supersonic shear layer. It was found that acoustically reflective surfaces, both downstream and below the shear layer, were essential for this resonance excitation to occur, and an upstream acoustically reflective surface augmented this excitation. However, none of these surfaces directly contacted the shear layer. Based on total pressure measurements, as much as 100% augmentation in mixing layer growth rate was achieved with this passive excitation system even at pressure matched conditions. Shadowgraph images of the shear layer showed the presence of singular coherent large-scale structures, and the acoustic spectra measured below the shear layer indicated the presence of a dominant frequency with overall high energy for the excited flow compared with a lower energy broadband spectrum for the unexcited flow. The results indicate that a combination of streamwise and transverse modes may be responsible for the excitation.

Introduction

RECENT interest in supersonic combustion (Scramjet) propulsion systems has resulted in extensive experimental and theoretical efforts to understand the compressible mixing process. Experimental and computational results¹⁻⁵ have shown that compressibility in such free shear layers (two stream and single stream) plays an important role in causing up to a fourfold reduction in mixing compared with the incompressible case at the same velocity and density ratios. To achieve an efficient Scramjet propulsion system, provisions for enhanced mixing are needed in short residence time combustors because of the reduced mixing at high Mach numbers caused by the inherent stability of such flows.

Several methods have been employed to study the possibility of mixing augmentation in compressible mixing layers. Increased mixing between supersonic reactant streams in chemical lasers has been achieved by essentially increasing the interfacial area between coflowing streams by using trip jets and ramp nozzles.⁶ Also, there have been several attempts to increase the fundamental mixing for flows with fixed interfacial area, including gasdynamic interaction, streamwise vorticity addition, acoustic excitation, etc.

One such gasdynamic interaction technique for mixing augmentation in supersonic streams is the shock-shear layer interaction. Strong shock waves cause increased turbulence downstream in the shear layer,⁷ which can aid in increasing the mixing. Also the misalignment of the pressure gradient and the density gradient caused by the impinging shock wave gives rise to baroclinic vorticity generation that may also augment mixing. The experimental work of Menon⁸ indicated that the shock-shear layer interaction coupled with a backward-facing step can be employed for this purpose. However, experiments conducted by Shau et al.⁹ and Ramaswamy et al.¹⁰ have shown that, for a two-dimensional shear layer, an oblique compression interaction yields only a local improvement in mixing augmentation. Also, strong shocks cause total pressure loss, which reduces the efficiency of the propulsion system.

A second technique to augment mixing is to add streamwise vorticity. Naughton and Settles¹¹ have shown that increased mixing between coflowing axisymmetric supersonic streams can be achieved by adding streamwise vorticity using vortex generators. Similarly, addition of streamwise vorticity using delta tabs¹² has resulted in a dramatic increase in axisymmetric jet mixing. However, addition of streamwise vorticity for the two-dimensional shear layer does not significantly improve mixing.^{13, 14} This lack of augmentation using

streamwise vorticity addition for planar shear layers may be related to the lack of helical instability modes that are present in the axisymmetric counterpart. For example, consider the two-dimensional subsonic stream experiments conducted by Bell and Mehta.¹⁵ In these mixing layers, the streamwise vortices are found to break up the growth of the large-scale spanwise vortices and can augment mixing only for a short downstream distance. But beyond a point, the mixing layer growth rate is reduced (sometimes even below the normal level), presumably because of the absence of entrainment by large spanwise structures present in the unperturbed mixing layers. These results indicate that, for increased mixing in high-speed two-dimensional shear layers, it may be more advantageous to strengthen the spanwise vortices for greater entrainment as opposed to streamwise vorticity addition.

A third augmentation technique is to use acoustic waves to excite the instability modes. Note that this technique differs from the standing gasdynamic wave interactions mentioned earlier in that we now consider acoustic waves that propagate with respect to the test section. Although active acoustic excitation has been widely used for subsonic planar shear layers, such excitation of the supersonic counterpart is not as common. One reason for this is that supersonic mixing layers require much higher amplitudes of perturbation, because of their inherent stability and high turbulence energy levels, to achieve any significant change in flow development. In recent active acoustic excitation experiments, Pimshtein¹⁶ excited an axisymmetric supersonic jet using high-intensity acoustic waves with sound pressure levels on the order of 162–170 dB. He concluded that the acoustic-supersonic jet interaction mechanism takes place close to the nozzle exit. Poldervaart et al.¹⁷ and Pimshtein¹⁶ have shown that the acoustic excitation of jet mixing layers is effective only when the waves are incident from the upstream quadrant, e.g., propagating normal to or in the streamwise direction. However, the energy levels required to actively excite the supersonic shear layer are extremely high.¹⁸ One potential method to overcome this difficulty may be to adopt passive excitation methods.

Glass¹⁹ investigated the effect of passive acoustic feedback on the spread rate of underexpanded sonic axisymmetric jets. The acoustic feedback loop consisted of screech tones generated by the jet (the screech tones are related to the length of shock cells), which travel upstream and are reflected close to the nozzle exit back into the jet by an acoustically reflective surface. He found that the reflected screech noise significantly altered the jet characteristics and yielded as much as a 50% increase in jet spread rate compared with the unexcited case. Recently, Yu et al.¹⁸ used a combination of a Mach 2 axisymmetric freejet and different size (both hemispherical and rectangular) cavities and obtained up to 90% augmentation in shear layer growth rate.

In all of the aforementioned studies on excitation, the flowfield was an axisymmetric freejet. In comparison, there are very few studies of planar shear layers that are bounded on one or more sides that

Received Oct. 2, 1995; revision received March 26, 1996; accepted for publication April 15, 1996. Copyright © 1996 by the American Institute of Aeronautics and Astronautics, Inc. All rights reserved.

*Postdoctoral Research Associate, Department of Mechanical and Industrial Engineering. Member AIAA.

†Associate Professor, Department of Aeronautical and Astronautical Engineering, 306 Talbot Laboratory. Senior Member AIAA.

have been passively excited. In bounded two-dimensional flows, the absence of flapping and helical instability modes can reduce the mixing layer growth rate. An example of a bounded flow geometry that has allowed aeroacoustic excitation is the cavity flow. Rossiter,²⁰ while studying the flow over rectangular cavities at subsonic and transonic speeds, found the presence of both random and periodic unsteady pressure components in the cavity. The shallower cavities were dominated by random components, whereas periodic components dominated the deeper cavities. Also, large-scale structures were found to be present in the shear layer formed over the cavities.

In this study, we examine the augmentation of a bounded supersonic planar shear layer with zero velocity ratio, at pressure matched conditions using tone excitation with acoustically reflective surfaces. These excited cases, at a minimum, require two acoustically reflective surfaces that are placed such that one forms a lower wall below the supersonic shear layer and the other is placed near the downstream end of the test section just above this wall, but not in the shear layer itself. The results show that the shear layer development is significantly affected by the acoustic feedback with the formation of large-scale structures resulting in as much as 100% augmentation in mixing layer growth rate compared with the unexcited case. We consider the results to be unique in that we were able to achieve very high mixing augmentation for a bounded two-dimensional shear layer without active excitation, by using resonance-based acoustically reflective surfaces, as opposed to only shock cell structure oscillations.

Experimental Method

The experiments were performed in a single-stream supersonic shear layer facility. The air for the supersonic jet is supplied from a tank farm that is fed from a compressor capable of supplying 33 m³/min of air at 7.8 atm. Since the compressor supply rate exceeds the airflow rate of the jet (0.5 kg/s), continuous operation of the wind tunnel is facilitated. The air is fed to the test section through a pneumatic regulator that maintains uniform flow conditions. The dimensions of the nozzle at the exit are 50 mm wide \times 13.5 mm high with a spatially uniform exit Mach number of 1.65 (verified with pitot surveys). The lower wall of the single-stream supersonic wind tunnel extends only to the splitter plate tip, with a trailing-edge thickness of 0.1 mm. The subsequent rectangular test section measures 100 mm long and 50 mm wide, with the bottom open to allow the entrainment of ambient air. Mixing was achieved between the supersonic stream above and the entrained air below. The Reynolds number of the flow based on the velocity difference and shear layer thickness based on shadowgraph images is 2.1×10^5 , at about 45 mm downstream from the splitter tip, which constitutes a fully turbulent shear layer.² In addition, the boundary layer itself is turbulent at the nozzle exit.²¹ The theoretical convective Mach number of the flow is about 0.74, and the relative Mach number is about 1.5 (see Ref. 21). Figure 1 shows the experimental setup with the relevant dimensions.

The initial objective of these passive excitation experiments was to excite the planar shear layer in a manner similar to that of Glass¹⁹ for an axisymmetric jet. As this configuration was not successful, we tried exciting the flow by placing an acoustically reflective sur-

face on the downstream side (based on the results of Pimshtein¹⁶ and Poldervaart et al.¹⁷). In this process, we noted that acoustic isolation by the addition of a lower wall was necessary for passive acoustic excitation to occur. Experiments with other configurations were performed to determine the germane features of this excitation in terms of necessary geometry and resulting flowfield characteristics.

The experimental setup in Fig. 1 shows the configuration for the baseline excited case, where passive excitation of the planar jet mixing layer was achieved by judiciously placing acoustically reflective surfaces near the flow. This consisted of an acoustically reflective lower wall and 19-mm cylinders downstream and upstream of the test section. The baseline unexcited case was achieved by simply removing the acoustically reflective lower wall and the cylinders. Several other geometry variations that were investigated include the removal of one or both of the cylinders, reducing the cylinder diameters (to either 13 or 6 mm) or replacing the cylinders with vertical flat plates (either 20 or 29 mm in height). Also, acoustic damping was achieved in these experiments by placing a sponge of 6-mm thickness over the lower wall or by the removal of the lower wall itself.

To study the effect of acoustic excitation on the shear layer, pitot probe measurements, shadowgraph photos, and acoustic pressure measurements were all taken for both the excited and unexcited baseline cases. The pitot probe was made by soldering a 6-mm-long 1.6-mm-diam tube to a 3-mm-diam tube that was connected to a pressure gauge. Several tests were conducted to ensure that the probe size was sufficiently small to avoid disturbing the shear layer evolution.²² The Rayleigh formula was used when the probe was in the supersonic stream and the isentropic relation was used when in the subsonic portion to compute the total pressures from the pitot probe data.

Instantaneous and multiple exposure shadowgraphs of the flow for several conditions were also obtained. The shadowgraph setup used was a standard one consisting of a xenon micropulser, spatial filter, a collimating lens, and a 35-mm camera. The instantaneous shadowgraphs were taken with a pulse of approximately 1- μ s duration. For the multiple exposure shadowgraph images, five of these light pulses were used for a single image.

The acoustic measurements inside the test section were made for different cases with a microphone head placed inside the test section at about 55 mm downstream of the splitter tip and 66 mm below the top wall, but just above the lower wall. The acoustic data acquisition consisted of a capacitance type microphone (ACO Pacific, Model 7016) with a built-in preamplifier (Model 4012), with a nearly constant frequency response up to 100 kHz. This frequency range was sufficient to find the most dominant frequency of the large-scale structures in the mixing layer. At least 32 ensembles with 2000 data points each were digitally sampled at 200 kHz for each case using an A/D board and IBM personal computer (details can be found in Ref. 22). Then the microphone data were digitally processed with a MATLAB Butterworth filter (with a coefficient of five and a bandpass between 100 Hz and 200 kHz). Based on the microphone frequency response and the filter frequency, only the spectrum between 200 Hz and approximately 75 kHz can be regarded with confidence. Thus, the acoustic measurements cannot provide details of the small-scale spectra. From MATLAB, the rms of the voltage for each of the ensembles and the power spectral density were obtained. The sound pressure level (SPL) in decibels was computed using a P_{ref} of 2×10^{-5} Pascal and the standard relationship

$$SPL = 20 \log_{10}(P_{rms}/P_{ref}) \quad (1)$$

Results and Discussion

Overall Observations of Excitation Geometries

This section is composed of simple auditory and visual observations (using shadowgraphs) of the effect of different configurations obtained with the acoustically reflective surfaces placed around the shear layer. We first discuss some of the unique observations made during these acoustic excitation experiments and compare them with similar previous studies. In this paper, excitation is defined as changes in the flow characteristics from the baseline unexcited case

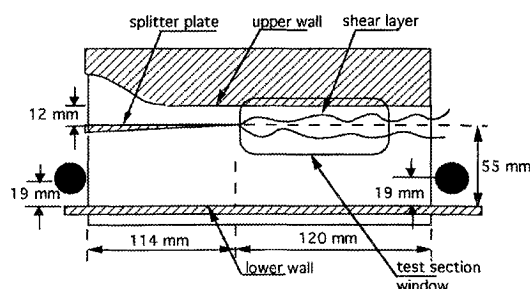


Fig. 1 Schematic of the experimental setup for the baseline excited case (both cylinders 19 mm in diameter).

in the form of appearance of distinct high-energy audible tones and a substantial increase in the shear layer thickness.

Glass¹⁹ and Jungowski²³ used acoustically reflective surface upstream of the nozzle of underexpanded jets to reflect the screech tones for exciting the flow. When we conducted similar experiments by placing an acoustically reflective plate upstream of the two-dimensional nozzle exit for both matched and unmatched exit pressure conditions, we did not observe any excitation for any angular orientations of the plate. The ineffectiveness of the screech mechanism in exciting this two-dimensional shear layer might be a result of the absence of either a helical mode or a jet flapping mode (since the present single-stream shear layer was bounded on all three sides) or because the upstream propagating screech tone was not strong enough to excite the flow. But when an acoustically reflective lower wall was employed along with a single 19-mm aluminum cylinder downstream and below the shear layer (as in Fig. 1 without the upstream cylinder), a high-amplitude single-tone frequency was clearly noted, and significant changes in the jet development were concurrently observed. The addition of a second cylinder upstream of the splitter tip (as shown in Fig. 1) further augmented the excitation. However, when the downstream cylinder was removed, with or without the upstream cylinder and the lower wall in place, no excitation was noticed. In addition, tests with the downstream cylinder in place (with or without the upstream cylinder) but no lower wall also resulted in no excitation. Note that both the downstream cylinder and the lower wall were placed significantly below the free shear layer (Fig. 1). Based on tests with several other configurations to be discussed later, it was determined that both an acoustically reflective lower wall and a downstream surface (e.g., cylinder or flat plate) were necessary for the excitation, whereas the second upstream surface only augmented this phenomenon.

Experiments similar to the baseline excited case were conducted by replacing the 19-mm-diam cylinder with a 12.5-mm-diam cylinder and flat plates of transverse height 20 and 30 mm. In all of the cases, excitation was observed at nearly the same tone, though the intensity increased with an increase in the size of the downstream acoustically reflective surface. A list of the different configurations tested and their effect on excitation is compiled in Table 1.

To investigate whether this effect was related to the interaction of eddies shed from the downstream cylinder by the entrained air, we extended the rear half of the downstream cylinder with a thickness equal to that of the cylinder diameter itself, for about 120 mm outside the test section. Even under this circumstance, the excitation was present and the tone was preserved. The insensitivity to the eddies shed from the downstream surface is consistent with the eddy shedding frequency being an order of magnitude lower than the observed excitation frequency.²² This frequency was found to be independent of the size and shape of this downstream reflecting plate as will be discussed later.

When the lower wall was covered with a 6-mm-thick sponge or when the downstream cylinder was covered with a sponge, the excitation was completely eliminated. When the downstream cylinder was placed such that it was in the supersonic stream, the excitation died out completely, and when it was in the shear layer, the excitation was highly attenuated. These experiments indicate that the downstream cylinder and the lower wall excite the flow based on their acoustically reflective properties.

Table 1 List of cases

Configuration type	Excitation	SPL (dB)
Baseline unexcited	No	134
Lower wall only (no cylinders)	No	140
Baseline excited with sponge	No	138
30-mm flat plate with sponge	No	— ^a
Two cylinders only	No	—
Baseline excited	Yes	161
20-mm flat plate	Yes	161
30-mm flat plate	Yes	—
Single cylinder + lower wall	Yes	158
12.5-mm cylinder	Yes	—

^aNot measured.

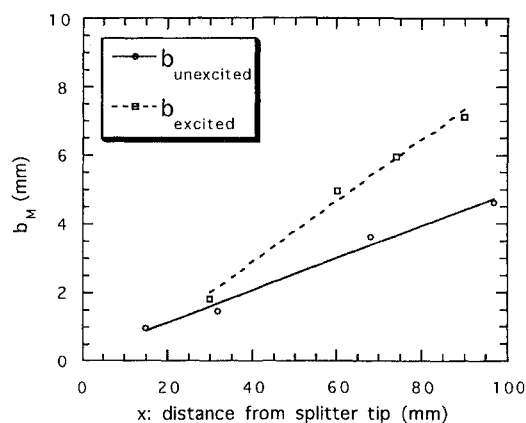


Fig. 2 Mixing layer thickness vs downstream distance (based on Mach number profile).

It was also observed that the single-tone excitation noise became audible only when the flow became supersonic but existed at roughly the same frequency for overexpanded, underexpanded, and matched exit pressure conditions. Therefore, quasi-steady-state shock cell oscillations present in the supersonic stream at unmatched exit pressure conditions are not necessary for this flow excitation (i.e., the conventional screech tone is not the primary excitation mechanism). Additional measurements to be discussed later showed that the changes in the distance from the splitter plate to either the lower acoustic wall or downstream cylinder yielded changes in the observed tone frequency. All of the preceding observations suggest that the mechanism involves an acoustic reflection propagating upstream or transversely in the subsonic flow below the shear layer and (as stated earlier) requires two acoustically reflective surfaces.

Stagnation Pressure Survey Results

The pitot probe data were also used to compute the Mach number profiles in the flow by using Rayleigh's equation in the supersonic portion of the flow and the isentropic relation in the subsonic section. A mixing layer thickness b_M was then defined based on the difference between the vertical positions where the Mach numbers were between 95 and 5% of the jet exit value. Based on the computed Mach number profiles, the shear layer thickness at various axial locations is plotted in Fig. 2. From this, we find that axial growth rate of both the baseline excited and unexcited cases to be linear, with the growth rate for the excited case being roughly twice that of the unexcited case. The growth rate for the unexcited case is about 40% of that for the incompressible case of comparable density and velocity ratios. Such a reduction in mixing layer growth rate for the compressible flow is consistent with those observed by several researchers at a relative Mach number of 1.5 (see Ref. 21 for details).

Spark Shadowgraph Studies

Spark shadowgraph images of the flowfield were made with various configurations as given in Table 1, where all of the experiments were conducted under pressure matched conditions. The results given next are based on several shadowgraph images for each configuration; however, for brevity, we present only a few example images herein. All of the shadowgraph images presented have markings at the bottom of the field of view (FOV) that coincide with the test section window of Fig. 1. Here the flow is from left to right. The largest vertical markings are at distances of 23, 46, 68, and 91-mm downstream from the splitter tip. Occasionally, the 23- and/or 91-mm markings are not visible.

Figure 3 shows a typical single-exposure shadowgraph image for the baseline unexcited case. The multitude of weak gasdynamic waves that are clearly visible starting from the left-hand side of the jet are a result of slight pressure mismatch (which was less than 1% of the ambient pressure) and small-scale turbulent structures causing weak expansion and compression waves crossing through the supersonic flow. Such small-amplitude waves are expected to have very little effect on the overall shear layer development.¹⁰ We also note



Fig. 3 Single-exposure shadowgraph of baseline unexcited case.

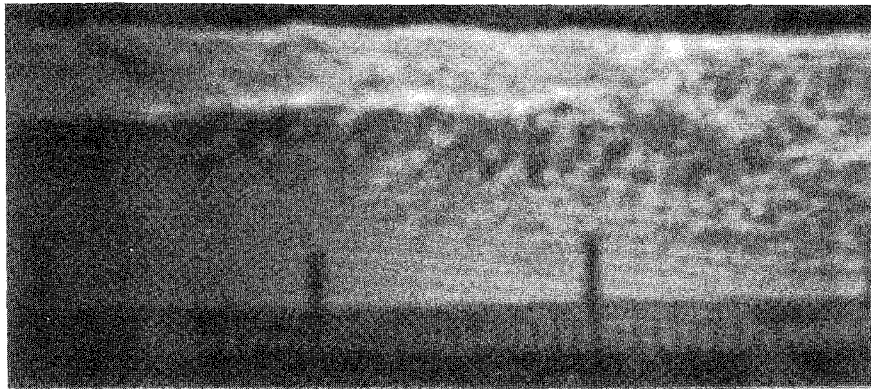


Fig. 4 Single-exposure shadowgraph of baseline excited case.

that a bright streak, which can be interpreted as an optical delineator for the sonic line (as evidenced by the termination of gasdynamic waves along this streak), is roughly horizontal and extends all of the way to the end of the FOV. This line is inclined slightly toward the upper wall, which is consistent with the streamwise decay of the supersonic core. The shear layer spreads more into the ambient air below where most of the turbulent structures are seen, than into the supersonic stream. The multiple-exposure shadowgraph for the unexcited case is very similar to this single-exposure shadowgraph showing a stable optical sonic line delineator that extends all of the way to the end of the FOV.²² The appearance of such a single sonic line delineator in the multiple-exposure shadowgraph indicates that this line did not undergo significant fluctuation, which is consistent with other studies where a planar jet was bounded on one side by a rigid wall. The only major difference of the multiple-exposure shadowgraph from the single-exposure shadowgraph was that the turbulent structures appear more diffused because of their superposition.

A single-exposure shadowgraph image for the baseline excited case is shown in Fig. 4. Two striking differences compared with the baseline unexcited case become evident from these figures. The first difference is that the jet spreads more compared with the baseline unexcited case (consistent with the pitot probe data). The second difference is that the optical sonic line delineator for the baseline excited case does not extend all of the way to the end of the FOV in contrast to the baseline unexcited case. It typically disappears at about 85-mm downstream from the splitter tip. In the multiple-exposure shadowgraph for this baseline excited case, we could clearly see at least two sonic lines emanating from the splitter tip.²² This shows that the excitation of the flow is coincident with strong vertical fluctuation of the shear layer. To our knowledge, this pseudoflapping has not been documented previously for a two-dimensional bounded shear layer.

To give further evidence that the excitation is caused by the downstream surface and the lower wall as noted in the preceding section, shadowgraphs were taken with the other configurations of Table 1. Often, a fairly large structure that resembles a forward inclined and elongated S can be seen in the mixing layer at various

streamwise locations. However, only one such large-scale structure was observed at any instant, which indicates that the wavelength between these structures is greater than the length of the FOV. It was noted that the large-scale S structures were found only for the conditions that also produced tone excitation, increased spread rates, and increased sound pressure levels. The size of the structures was found to increase with increasing downstream reflective surface area (consistent with additional acoustic blockage). For example, Figs. 5–7 show single-exposure shadowgraphs for the configuration using the 30-mm flat plates taken at different instances indicating strongly unsteady flow. All three images show large-scale vortical structures in the mixing layer at various streamwise positions, where we note their increased size as they convect downstream. In Fig. 5, we can see a small vortical structure at about 45-mm downstream from the splitter tip; it is presumably in the early stage of its development. In Fig. 6, we can see a well-developed large-scale structure at about 60-mm downstream from the splitter tip, downstream of which small-scale structures are especially pervasive and what appears to be an oblique shock angled to the upper wall. The appearance of an oblique shock may be caused by flow locally expanding just above the structure and then shocking to meet the ambient pressure condition. Usually in these figures, the mixing layer has the largest thickness around the location where this large structure forms. It is difficult to determine the quantitative aspects of the large-scale structure interaction with the top wall, but no boundary-layer separation on the top wall was observed in the shadowgraphs. However, strong streamwise pressure gradients are expected to occur as a result of the large-scale structure presence.

Acoustic Pressure Measurements

The acoustic measurements near the lower wall were also obtained for several configurations. The oscilloscope trace of the microphone response for the baseline unexcited case is shown in Fig. 8 at 1 V/div and 1 ms/div resolution, where a broadband-type signal is evident. In contrast, the baseline excited case with the same temporal resolution (Fig. 9) shows obvious periodicity at about 3 kHz



Fig. 5 Single-exposure shadowgraph of 30-mm flat plate excited case.

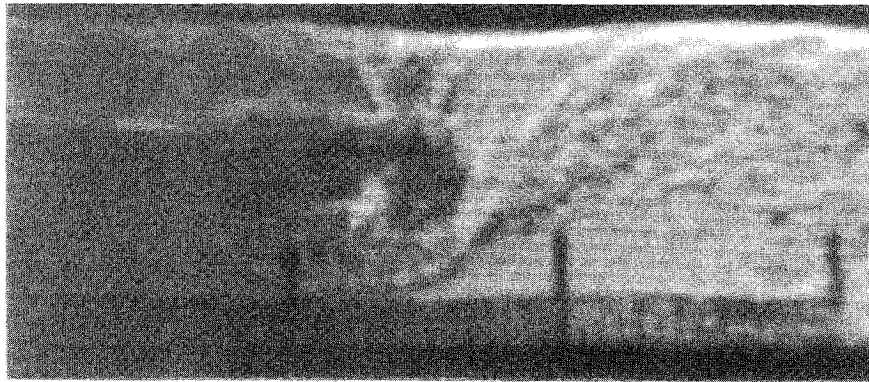


Fig. 6 Single-exposure shadowgraph of 30-mm flat plate excited case.

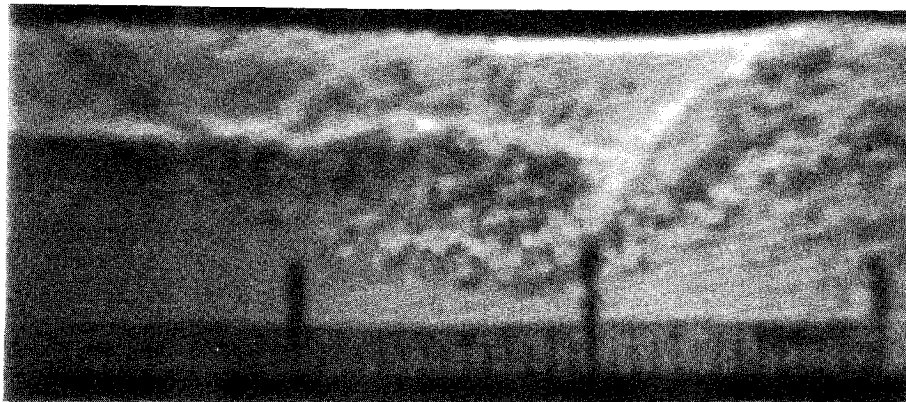


Fig. 7 Single-exposure shadowgraph of 30-mm flat plate excited case.

with a much greater amplitude (5 V/div was used for this trace). The details of this signal are shown with a higher resolution of 0.1 ms/div in Fig. 10. Nearly constant periodicity and high amplitude were found only for those configurations that yielded tone excitation. The traces for the excited cases were also characterized by a relatively sharp rise followed by a slower fall. This is consistent with the propagation of a strong acoustic wave (with a steepening of the compression portion) in the region below the shear layer. The baseline excited case shows a three decade increase in sound pressure level (161 dB) as compared with the unexcited case (134 dB). When the excitation configuration was damped with a sponge over the lower wall, the sound pressure level dropped to 138 dB, which is consistent with other nonexcited cases (see Table 1).

The power spectra of the microphone output inside the test section for the baseline unexcited and excited cases are shown in Fig. 11. For the unexcited case, we obtain a spectrum with two moderate

peaks, with one at 1 kHz and the other at 3 kHz. Above 3 kHz, we see a broadband spectrum with almost a uniform amplitude up to 35 kHz, beyond which the spectrum drops off sharply. In contrast, the baseline excited case clearly shows a dominant frequency centered around 3 kHz (which is comparable to the 2.93 kHz obtained directly from the fast Fourier transform of the digital oscilloscope). Several well-defined higher harmonics of this frequency with the amplitude decreasing monotonically are also seen. These harmonic peaks have magnitudes that are several orders of magnitude higher than any of the unexcited cases. The higher harmonics exist up to a frequency of about 20 kHz, and after that, only a broadband spectrum, which drops off sharply as in the unexcited case after 35 kHz, is seen. Based on the acoustic spectra, the ratio of the mean square pressure fluctuations, between the baseline excited case and the unexcited case at 3 kHz, is about 5400. However, the ratio over the whole frequency range is about 500.

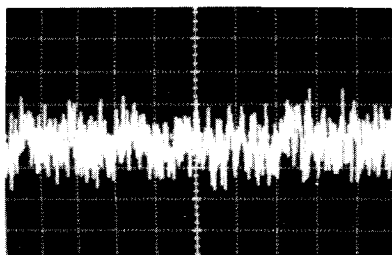


Fig. 8 Oscilloscope trace of the microphone response for the baseline unexcited case; the vertical scale is 1 V/div and horizontal scale is 1 ms/div.

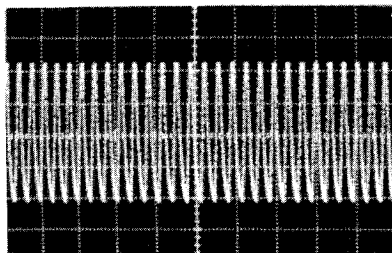


Fig. 9 Oscilloscope trace of the microphone response for the baseline excited case; the vertical scale is 5 V/div and horizontal scale is 1 ms/div.

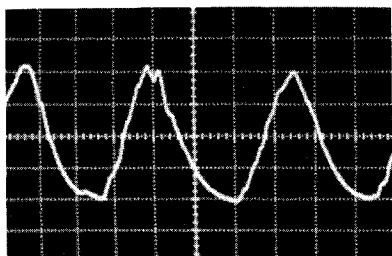


Fig. 10 Oscilloscope trace of the microphone response for the baseline excited case; the vertical scale is 5 V/div and horizontal scale is 0.1 ms/div.

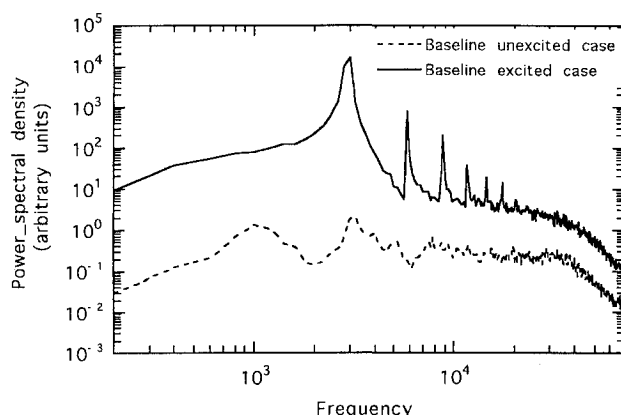


Fig. 11 Acoustic power spectra for the baseline unexcited and excited cases.

This general behavior delineating the excited from the unexcited cases was consistent with the spectra obtained for other conditions.²² However, the single downstream cylinder excited case was different from the baseline excited case by the absence of all but the first higher harmonic. The addition of the upstream cylinder might have enhanced the acoustic excitation below the shear layer by additional acoustic isolation.

Potential Aeroacoustic Mechanisms

The aeroacoustic mechanism responsible for the passive excitation is not obvious in that there are no previous studies that have investigated an equivalent flow geometry. Blake and Powell²⁴ categorized the different sets of commonly observed flow–acoustic interactions. The type of flow interactions observed in our experiment do not strictly fall under any of the categories mentioned therein. More recently, Gutmark et al.²⁵ reviewed many of the passive aeroacoustic excitation schemes for supersonic shear flows, but these were again for different flow configurations (primarily axisymmetric freejets). To consider the potential mechanisms, we first note that the present experiments established that plate or cylinder shedding was not critical to this excitation mechanism and that the upstream plate or cylinder merely enhanced the excitation (presumably by decreasing acoustic pressure leakage) and was not essential. Therefore, for the remainder of the discussion, the influence of this upstream reflective surface and the shape of the downstream surface (nominally a cylinder) will not be addressed.

As the excitation was initiated only when the flow was supersonic, conventional screech tone excitation resulting from shock cell oscillations was a candidate for the aeroacoustic interaction. However, screech is proportional to shock cell size²⁵ and therefore varies in frequency and strength as the level of exit pressure mismatch varies. Since the present acoustic interaction at pressure matched conditions was roughly as strong as at unmatched conditions and since the primary excitation frequency was preserved at all exit conditions (various degrees of underexpanded and overexpanded pressure mismatches), conventional screech as the excitation mechanism was ruled out. Also, for a conventional screech excitation, a downstream acoustically reflective surface is not necessary as the screech tone travels upstream.

A more promising possibility is that of an acoustic mode that travels vertically between the shear layer and the lower wall. In this respect, it should be noted that Yu et al.¹⁸ conducted experiments on the excitation of an axisymmetric supersonic jet stream by a two-dimensional cavity placed near the nozzle exit and found the depth of the cavity to be an important parameter that affects the excitation mechanism. Also, Abdel-Fattah and Favaloro²⁶ found that transverse modes of duct resonance affected ejector performance significantly. Although these experiments were conducted with axisymmetric freejets for which flapping, helical, and contraction/expansion modes were possible, the aforementioned evidence of pseudoflapping and the importance of the lower wall in causing the excitation in the current experiments indicate transverse acoustic modes may be important.

Another possibility is that of an acoustic mode that convects with the shear layer and then travels upstream below the shear layer where the flow is nearly quiescent. This is consistent with the upstream propagation mechanism cited for jet screech¹⁹ for which the flow leaving the splitter plate is known to be especially susceptible to acoustic disturbances. Note that this mechanism seems far more likely than upstream propagation along the upper wall supersonic boundary layer. In this regard, the present configuration has similar acoustic features as that of Rossiter's²⁰ configuration of transonic flow over a cavity; i.e., both have an acoustically reflective downstream surface and a high-speed flow that separates from an upstream edge. However, we note that Rossiter's experiments had no entrained flow and the shear layer was essentially terminated at the end of the cavity. The importance of the downstream acoustically reflective surface and the observed convection of large coherent structures in our experiments suggests that a streamwise mode similar to that proposed for a cavity-driven excitation is possible.

Figure 12 shows a schematic of the proposed aeroacoustic streamwise model that is consistent with the measurements made in this study. This model consists of an eddy-generated pressure disturbance that convects downstream, then reflects off the downstream plate or cylinder, and then propagates upstream as an acoustic disturbance through the subsonic entrained flow below to trigger another eddy disturbance. For the streamwise mode, let us assume that large coherent eddies in the shear layer travel at k fraction of the freestream speed U_1 . Let us also assume that the disturbance generated by the eddy in the shear layer reflects from the downstream cylinder at time

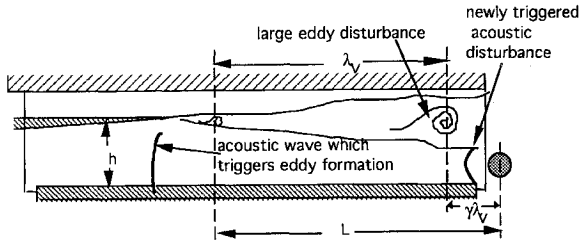


Fig. 12 Schematic of the plausible aeroacoustic excitation mechanism.

$t = 0$ when the eddy is at a distance of $\gamma\lambda_v$ upstream of the cylinder as shown in Fig. 12, where λ_v is the wavelength of the eddies convecting in the shear layer and γ is an arbitrary constant that defines the fraction of the vortex wavelength distance from the downstream cylinder upon which acoustic reflection occurs. Note that γ is positive if this occurs when the eddy is upstream and negative if it is downstream of the cylinder. An important criterion for streamwise excitation is that the frequency of eddy generation is the same as the dominant frequency of the upstream propagating acoustic wave (ω_s), i.e.,

$$\omega_s = \frac{kU_1}{\lambda_v} = \frac{a_2 - U_2}{\lambda_a} \quad (2)$$

where λ_a is the wavelength of the acoustic waves and a_2 is the speed of sound in the entrained air (below the shear layer).

This disturbance, which is initiated at the downstream cylinder by the eddy, propagates upstream and reaches the splitter tip at time $t_a = L/(a_2 - U_2)$ where L is the distance of the downstream cylinder from the splitter tip. During this time, the initial eddy travels downstream a distance $kU_1 L/(a_2 - U_2)$. Therefore, the wavelength of the eddies can be given by the relation

$$n_s \lambda_v = L - \gamma \lambda_v + \frac{kU_1 L}{a_2 - U_2} \quad (3)$$

where n_s is the streamwise mode number defined as the total number of perturbations present at a given time and the perturbations can include both eddies in the shear layer and acoustic waves below (n is an integer with a minimum value of unity). For example, $n_s = 1$ means that only a single acoustic wave or a single large eddy will exist in the test section at a given instant. In Fig. 12, $n_s = 2$ such that while one acoustic wave is triggering a new eddy, a previous eddy is triggering a new acoustic wave at the downstream cylinder. Note that the experimental results that showed only one eddy in the FOV at any given instant are consistent with a maximum n_s of 4, since the FOV is approximately $L/2$. The pitot probe measurements indicate that $U_2 \ll a_2$; therefore, the wavelength of the eddies is

$$\lambda_v = \left(1 + \frac{kU_1}{a_2}\right) \frac{L}{(n_s + \gamma)} \quad (4)$$

Substituting this in the relation for the frequency of the eddies, we obtain

$$\omega_s = \frac{kU_1}{L} \frac{(n_s + \gamma)}{[1 + (kU_1/a_2)]} \quad (5)$$

Rossiter²⁰ suggests $k = \frac{2}{3}$ for his cavity flow. For the present supersonic free shear layer conditions, we use the average nonexcited convection speed obtained from temporal correlations of Mie-scattering movies²¹ yielding a k of approximately 0.76. Substituting this into Eq. (5) for $n_s = 2$ and $U_1 = 469$ m/s yields a γ of -0.003 for the acoustically measured frequency (ω_m) of 2.93 kHz. This is consistent with an acoustic wave reflection being sent upstream of the cylinder at nearly the same time the large eddy reaches the cylinder location. This small value seems reasonable since the convection speed of the eddy is transonic with respect to the quiescent flow below and the pressure disturbance created by it (with respect to the entrained flow below the shear layer) cannot travel at a higher speed.

Table 2 Frequencies for various geometries

L , mm	h , mm	n_s	n_t	ω_s , kHz	ω_t , kHz	ω_m , kHz
120	55	2	1	2.93	3.09	2.93
155	55	3	1	3.37	3.09	3.09
155	65	2	1	2.22	2.61	2.19

Now let us consider the transverse modes. We may write a simple relationship for the transverse frequency ω_t based on the distance between the shear layer and the lower wall surface, which we will approximate herein as the distance between the splitter plate and the lower wall h ,

$$\omega_t = a_2(n_t/2h) \quad (6)$$

where n_t is the number of transverse acoustic waves present at any given time. The baseline excited configuration with $n_s = 1$ and $h = 55$ mm yields $\omega_t = 3.09$ kHz, which also agrees well with the measured frequency for this case. This suggests that both transverse and streamwise modes may be responsible of the excitation.

To investigate this further, we conducted two more excitation tests where h and L were independently varied and where the measured frequency ω_m was compared with ω_s and ω_t for n_s and n_t specified to be the closest integer value to match the measured frequency. These results are compiled in Table 2. It appeared that, for these few cases, excitation occurred when integer values of n_s and n_t yielded ω_s and ω_t within at least 15% of each other. The consistency of $n_t = 1$ for these tests is presumably a consequence of a shorter time period for a full transverse cycle compared with a full streamwise cycle. These results, coupled with the observation that both an acoustically reflective lower surface and a downstream surface were necessary for the tone excitation, suggest that the tone excitations observed in this study are a result of normal and streamwise modes coupling together. However, to confirm this hypothesis, more detailed fundamental investigations are needed, such as systematically varying the geometric and flow parameters as well as multiple microphone measurements to obtain acoustic propagation speeds and directions.

Conclusions

The present measurements clearly demonstrated the feasibility of passive acoustic excitation for augmentation of two-dimensional bounded supersonic shear layers. By properly placing the acoustically reflective surfaces, nearly 100% augmentation in shear layer entrainment was achieved along with the production of highly periodic acoustic waves that yielded sound pressure levels typically 30 dB higher than the unexcited case. The shadowgraph images and the near-field acoustic spectra below the shear layer showed the excited shear layer development to be a highly dynamic phenomenon. The size of the large-scale structures in the shear layer and its spread was found to depend on the size of the downstream acoustic reflective surface and was also correlated with increased sound pressure levels. The experiments that varied the streamwise and transverse distances of the acoustically reflective plates indicate that the excitation is a complex phenomenon that depends on both the transverse and streamwise modes of acoustic propagation.

References

- Papamoschou, D., and Roshko, A., "The Compressible Turbulent Shear Layer: An Experimental Study," *Journal of Fluid Mechanics*, Vol. 197, Dec. 1988, pp. 453–477.
- Goebel, S. G., and Dutton, J. C., "Experimental Study of Compressible Turbulent Mixing Layers," *AIAA Journal*, Vol. 29, No. 4, 1991, pp. 538–546.
- Burr, R. F., and Dutton, J. C., "Numerical Simulations of Compressible and Reacting Temporal Mixing Layers and Implications for Modeling," AIAA Paper 91-1718, June 1991.
- Oh, C. K., and Loth, E., "Finite Element Simulation of Supersonic Mixing Layer," AIAA Paper 92-3438, July 1992.
- Birch, S. F., and Eggers, J. M., "A Critical Review of the Experimental Data for Developed Free Turbulent Shear Flows," NASA SP-321, July 1972.
- Driscoll, R. J., "Mixing Enhancement in Chemical Lasers. Part I: Experiments," *AIAA Journal*, Vol. 24, No. 7, 1986, pp. 1120–1126.

- ⁷Zang, T. A., Hussaini, M. Y., and Bushnell, D. M., "Numerical Computations of Turbulent Amplification in Shock-Wave Interactions," *AIAA Journal*, Vol. 22, No. 1, 1984, pp. 13-21.
- ⁸Menon, S., "Shock-Wave-Induced Mixing Enhancement in Scramjet Combustors," AIAA Paper 89-0104, Jan. 1989.
- ⁹Shau, Y. R., Dolling, D. S., and Choi, K. Y., "Organized Structure in a Compressible Turbulent Shear Layer," *AIAA Journal*, Vol. 31, No. 8, 1993, pp. 1398-1405.
- ¹⁰Ramaswamy, M., Loth, E., and Dutton, J. C., "Free Shear Layer Interaction with an Expansion-Compression Wave Pair," *AIAA Journal*, Vol. 34, No. 3, 1996, pp. 565-571; see also AIAA Paper 95-0475, Jan. 1995.
- ¹¹Naughton, J. W., and Settles, G. S., "Experiments on the Enhancement of Compressible Mixing via Streamwise Vorticity, Part I—Optical Measurements," AIAA Paper 92-3549, July 1992.
- ¹²Samimy, M., Zaman, K. B. M. Q., and Reeder, M. F., "Supersonic Jet Mixing Enhancement by Vortex Generators," AIAA Paper 91-2263, June 1991.
- ¹³Papamoschou, D., "Structure of the Compressible Turbulent Shear Layer," AIAA Paper 89-0126, Jan. 1989.
- ¹⁴Dolling, D. S., Fournier, E., and Shau, Y. R., "Effects of Vortex Generators on the Growth Rate of a Compressible Turbulent Shear Layer," AIAA Paper 90-1979, July 1990.
- ¹⁵Bell, J. H., and Mehta, R. D., "Effects of Imposed Spanwise Perturbations on Plane Mixing-Layer Structure," *Journal of Fluid Mechanics*, Vol. 257, Dec. 1993, pp. 33-63.
- ¹⁶Pimshtein, V. G., "Disturbance Generation in Supersonic Jets Under Acoustic Excitation," *AIAA Journal*, Vol. 32, No. 7, 1994, pp. 1345-1349.
- ¹⁷Poldervaart, L. J., Winjnads, A. P., and Bronkhorst, L., "Aerosonic Games with the Aid of Control Elements and Externally Generated Pulses,"

AGARD-CP-131, Sept. 1973, pp. 20-1-20-4.

¹⁸Yu, K., Gutmark, E., Smith, R. A., and Schadow, K. C., "Supersonic Jet Excitation Using Cavity-Actuated Forcing," AIAA Paper 94-0185, Jan. 1994.

¹⁹Glass, D. R., "Effects of Acoustic Feedback on the Spread and Decay of Supersonic Jets," *AIAA Journal*, Vol. 6, No. 10, 1968, pp. 1890-1897.

²⁰Rossiter, J. E., "Wind-Tunnel Experiments on the Flow over Rectangular Cavities at Subsonic and Transonic Speeds," Aeronautical Research Council, Rept. and Memo. 3438, Oct. 1964, London.

²¹Mahadevan, R., and Loth, E., "High-Speed Cinematography of Compressible Mixing Layers," *Experiments in Fluids*, Vol. 17, No. 3, 1994, pp. 179-189.

²²Ramaswamy, M., "Gasdynamic and Acoustic Interactions with Supersonic Free Shear Layers," Ph.D. Thesis, Dept. of Aeronautical and Astronautical Engineering, Univ. of Illinois at Urbana-Champaign, IL, 1994.

²³Jungowski, W. M., "Influence of Closely Located Solid Surfaces on the Sound Spectra Radiated by Gas Jets," *Mechanics of Sound Generation in Flows*, edited by E. A. Muller, IUTAM/ICA/AIAA-Symposium, Gottingen, Germany, Springer-Verlag, Berlin, 1979.

²⁴Blake, W. K., and Powell, A., "The Development of Contemporary Views of Flow-Tone Generation," *Proceedings of an International Symposium, Recent Advances in Aeroacoustics*, edited by A. Krothapalli and C. A. Smith, Springer-Verlag, Berlin, 1983.

²⁵Gutmark, E. J., Schadow, K. C., and Yu, K. H., "Methods for Enhanced Turbulence Mixing in Supersonic Shear Flows," *Applied Mechanics Review*, Vol. 47, No. 6, Pt. 2, 1994, pp. S188-S192.

²⁶Abdel-Fattah, A. M., and Favaloro, S. C., "Duct Resonance and Its Effect on the Performance of High-Pressure Ratio Axisymmetric Ejectors," *AIAA Journal*, Vol. 26, No. 7, 1988, pp. 791-798.

Global Positioning System: Theory and Applications

Bradford W. Parkinson and James J. Spilker Jr., editors, with Penina Axelrad and Per Enge

This two-volume set explains the technology, performance, and applications of the Global Positioning System (GPS). This set is the only one of its kind to present the history of GPS development, the basic concepts and theory of GPS, and the recent developments and numerous applications of GPS. Volume I concentrates on fundamentals and Volume II on applications.

Each chapter is authored by an individual or group of individuals who are recognized as leaders in their area of GPS. These various viewpoints promote a thorough understanding of the system and make *GPS—Theory and Applications* the standard reference source for the Global Positioning System.

The texts are recommended for university engineering students, practicing GPS engineers, applications engineers, and managers who wish to improve their understanding of the system.

1995

Vol. I, 694 pp, illus,
Hardback
ISBN 1-56347-106-X
AIAA Members \$69.95
Nonmembers \$89.95
Order #: V-163(945)

Vol. II, 601 pp, illus,
Hardback
ISBN 1-56347-107-8
AIAA Members \$69.95
Nonmembers \$89.95
Order #: V-164(945)

Complete set
AIAA Members \$120
Nonmembers \$160
Order #: V-163/164(945)



American Institute of Aeronautics and Astronautics

Publications Customer Service, 9 Jay Gould Ct., P.O. Box 753, Waldorf, MD 20604
Fax 301/843-0159 Phone 1-800/682-2422 8 a.m. - 5 p.m. Eastern

CONTENTS:

Volume I.

Part 1. GPS Fundamentals

Introduction and Heritage and History of NAVSTAR, the Global Positioning System • Overview of the GPS Operation and Design • Signal Structure and Theoretical Performance • GPS Navigation Data • GPS Satellite Constellation and GDOP • GPS Satellite and Payload • Signal Tracking Theory • GPS Receivers • Navigation Algorithms and Solutions • GPS Control Segment

Part 2. GPS Performance and Error Effects

GPS Error Analysis • Ionosphere Effect • Tropospheric Effects • Multipath Effects • Foliage Attenuation for Land Mobile Users • Ephemeris and Clock Navigation Message Accuracy • Selective Availability • Relativistic Effects • Joint Program Office Test Results • Interference Effects and Mitigation

Volume II.

Part 1. Differential GPS and Integrity Monitoring

Differential GPS • Pseudolites • Wide Area DGPS • Wide Area Augmentation System • Receiver Autonomous Integrity Monitoring

Part 2. Integrated Navigation Systems

GPS/Loran • GPS/Inertial Integration • GPS/Barometric Altimeter • GPS/GLONASS

Part 3. GPS Navigation Applications

Land Vehicle Navigation and Tracking • Marine Applications • Air Traffic Control and Collision Avoidance • General Aviation • Aircraft Approach and Landing • Kinematic • Closed Loop Space Applications

Part 4. Special Applications

Time Transfer • Survey • Attitude Determination • Geodesy • Orbit Determination • Test Range Instrumentation

Sales Tax: CA residents, 8.25%; DC, 6%. For shipping and handling add \$4.75 for 1-4 books (call for rates for higher quantities). Orders under \$100.00 must be prepaid. Foreign orders must be prepaid and include a \$20.00 postal surcharge. Please allow 4 weeks for delivery. Prices are subject to change without notice. Returns will be accepted within 30 days. Non-U.S. residents are responsible for payment of any taxes required by their government.